ELSEVIER

Journal of Power Sources 68 (1997) 333–337

JOURNAL OF POWER SOURCES

In situ Raman spectroscopic study of Li_xCoO_2 electrodes in propylene carbonate solvent systems

Takashi Itoh, Hajime Sato, Tatsuo Nishina, Tomokazu Matue, Isamu Uchida

Department of Applied Chemistry, Graduate School of Engineering, Tohoku University, Aramaki-Aoba, Aoba-ku, Sendai 980-77, Japan

Accepted 6 December 1996

Abstract

Simultaneous measurements of in situ Raman spectroscopy and cyclic voltammetry have been carried out for thin film electrodes of Li_xCoO_2 in propylene carbonate containing 1 M $LiClO_4$. The Raman lines of 485 and 587 cm^{-1} observed at Li_xCoO_2 electrodes were attributed to the A_{1g} and E_g modes of the $LiCoO_2$, respectively. The Raman intensity of two lines changed drastically during the insertion/extraction of lithium ions. This effect can be explained by the reduction of the optical skin depth due to the conductivity change of Li_xCoO_2. Phase transition from Raman-active phase to Raman-inactive phase is also conceivable. © 1997 Elsevier Science S.A.

Keywords: Raman spectroscopy; Cobalt; Lithium secondary batteries; Optical skin depth; Lithium intercalation; Lithium insertion

1. Introduction

Raman spectroscopy has been used extensively to study the microscopic features of electrochemical reactions. Raman spectroscopy coupled with electrochemistry, i.e. in situ Raman spectroscopy has also been a powerful tool to study the electrochemical reaction. Moreover, when SERS (surface enhanced Raman scattering) effect is used, the Raman intensity of adsorbed molecules on the electrode surface is enhanced by a factor of 10^5–10^6 compared with that of free molecules [1].

The application of in situ Raman spectroscopy to carbon materials such as highly oriented pyrolytic graphite (HOPG) and natural graphite was investigated extensively in aqueous [2] and in organic solutions [3,4]. Lithium surfaces in organic solvents were also studied by in situ Raman [5,6] and in situ Fourier-transform infrared (FT-IR) [7,8] spectroscopies.

The lithium intercalation/ de-intercalation processes of Li_xCoO_2 involving a phase transition during charging/discharging have been investigated so far by using X-ray diffraction (XRD) [9,10]. However, XRD measurements give only limited information on the lithium site in the crystal structure, because the atomic scattering factor of lithium is much smaller than that of cobalt. By contrast, in situ Raman spectroscopy is very sensitive to the symmetry of structure near the surface region, and affords the vibrational information on molecules at the interface where the reaction is taking place. Therefore, in situ Raman spectroscopy is particularly suitable for the molecular-level investigation of intercalation/de-intercalation processes. However, in situ Raman studies of cathode materials for lithium batteries have been reported scarcely.

In the present study, we report here in situ Raman spectroscopic investigation of thin film Li_xCoO_2 electrodes. It is demonstrated that the variation of Raman spectra with electrode potential was obtained simultaneously with cyclic voltammograms (CV) under potentiostatic conditions.

2. Experimental

The measurements were carried out in an air-tight Pyrex electrochemical cell having three-electrode configuration. An optically flat sapphire window was used for the laser incident portion of the electrochemical cell. The working electrode was a thin film Li_xCoO_2 (5 mm diameter and about 0.2 μm thick) prepared on a gold substrate. Details of the preparation procedure of this electrode were reported elsewhere [11]. The Raman lines associated with Li_xCoO_2 were identified by comparing the sample with powdered Li_xCoO_2 prepared by the citrate process [12]. The lithium foils on a nickel mesh were used as the counter and reference electrodes. The cell was assembled in an argon-filled dry box (Miwa, MDB-1B + MS-P15S). Electrochemical measurements were performed with a Solartron 1267 potentiostat coupled with

PII S0378-7753(97)02539-1

Corrware for Windows (Scribner Associates) at room temperature (22±2 °C). The measurements started after the electrode potential was settled to open-circuit potential, then the potential of $LiCoO_2$ electrode was scanned between 3.1 and 4.2 V versus Li/ Li^+. The electrolyte solution was propylene carbonate (PC) containing 1 M $LiClO_4$ (Mitsubishi Chemical).

The argon-ion laser (Coherent, Innova 70) radiation (514.5 nm, 50 mW) was directed to the working electrode surface with an incident angle of about 60°. It was focused on the working electrode surface with a spot size of about 0.1 mm × 1.0 mm. The scattered light was collected and focused on the entrance slit of a triple-stage spectrograph (Jasco, TRS-300). The entrance slit width of the spectrograph is 400 μm.

In situ measurements of Raman spectra were performed with a diode array detector (Hamamatsu Photonics, M2493) with an intensifier (Hamamatsu Photonics, M2492) and controlled by a PMA (photo multichannnel analyzer) console (Hamamatsu Photonics, C2491) and a personal computer (NEC, PC-9801DA). Our system acquired a Raman spectrum of 2400 or 800 cm^{-1} in 512 data points. The Raman spectra were taken in every 75 s for data accumulation. The wavenumber of channel number of the diode array was decided by the luminescence of a neon lamp, and the wavelength dependence of our measurement system was corrected with a tungsten lamp. It is possible to obtain the electrochemical in situ Raman spectra with time resolution of seconds.

3. Results

3.1. Cyclic voltammetry

Fig. 1 shows a typical CV at 0.1 mV/s for a thin Li_xCoO_2 film electrode. Anodic and cathodic current peaks were observed at 4.0 and 3.83 V, respectively. The anodic peak is attributed to the de-intercalation of lithium from Li_xCoO_2 and the cathodic peak is due to the intercalation of lithium to Li_xCoO_2. This voltammetric result is almost consistent with those reported in the literature [11]. During CV, we carried out in situ Raman spectroscopic measurements. To avoid the interference by Raman signals from the solution side species, we pressed the film electrode onto the optical window to eliminate the organic solvent between the window and the electrode surface. The distortion of the CV is mainly caused by the increased solution resistance present in the window gap.

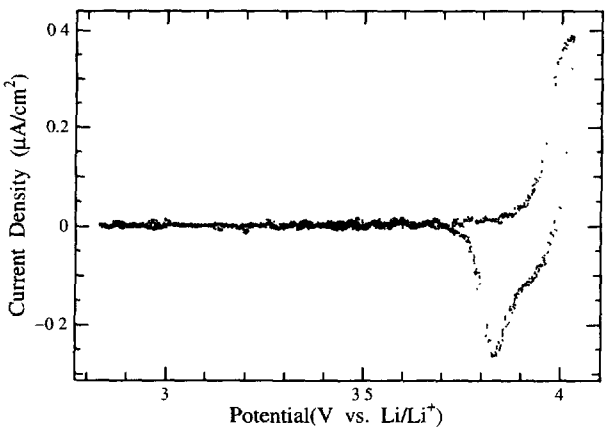

Fig. 1. Cyclic voltammogram of thin film of Li_xCoO_2 electrodes on gold; scan rate is 0.1 mV/s.

3.2. Ex situ Raman spectra of $LiCoO_2$

Before the in situ measurements, we examined ex situ Raman spectra of $LiCoO_2$ as shown in Fig. 2(a) powder and (b) thin film $LiCoO_2$ on gold substrate. Strong Raman lines were observed at 485 and 597 cm^{-1} in Fig. 2(a), and at 475 and 590 cm^{-1} in Fig. 2(b). The space group of $LiCoO_2$ is $R3m$ (D^5_{3d}) with $Z=1$ and the total vibrational modes of an $LiCoO_2$ unit cell are $A_{1g}+E_g+2A_{2u}+2E_u$. The A_{1g} and E_g modes are Raman-active, and the $2A_{2u}$ and $2E_u$ modes are IR-active [13]. The Raman spectrum of the powder was found to be identical with that reported by Inaba et al. [14], and the lines at 485 and 597 cm^{-1} are assigned respectively to the A_{1g} and E_g modes.

Although the spectrum of the $LiCoO_2$ film is slightly different from that of the powder, the Raman lines at 475 and 590 cm^{-1} are well definable, showing sharp peaks and assigned to the A_{1g} and E_g mode of $LiCoO_2$, respectively. Difference in the frequency and the peak width may be attributed to the difference in the preparation procedure of $LiCoO_2$. Crystallinity of the film sample seemed to be better than the powder sample.

3.3. In situ Raman spectra

Figs. 3 and 4 show the Raman spectra of Li_xCoO_2 electrodes in PC containing 1 M $LiClO_4$ in the frequency 250–1050 cm^{-1} range, during potential cycling between 3.1 V (open circuit) and 4.2 V. At the open-circuit potential (3.1 V), many Raman lines were observed in the spectrum. The Raman lines of 485 cm^{-1} (A_{1g}) and 597 cm^{-1} (E_g) are

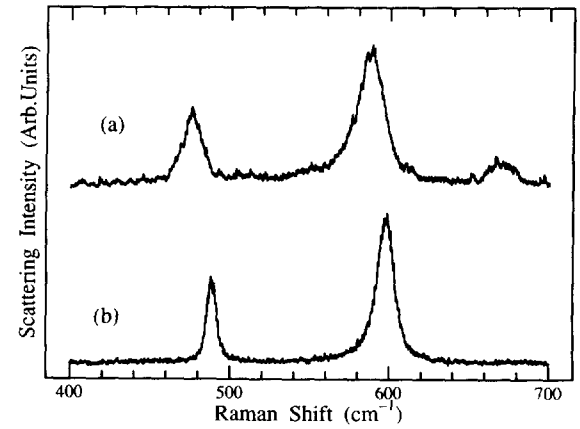

Fig. 2. Variation of Raman spectra of (a) powder and (b) thin film of $LiCoO_2$ on gold flags.

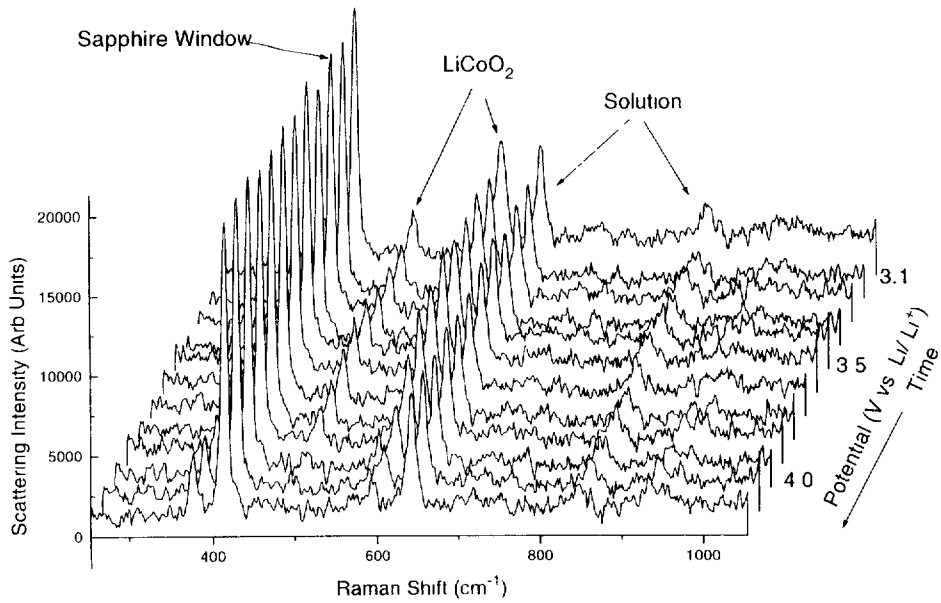

Fig. 3. Raman spectra of Li_xCoO_2 electrodes on a gold flag in PC containing 1 M $LiClO_4$ with increasing potential; scan rate is 0.1 mV/s.

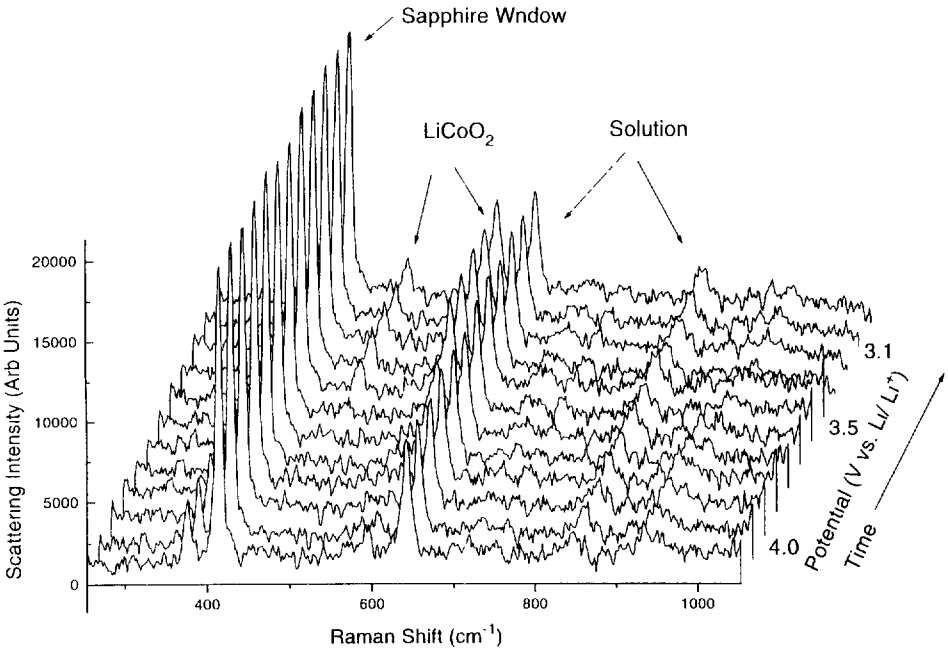

Fig. 4. Raman spectra of Li_xCoO_2 electrodes on a gold flag in PC containing 1 M $LiClO_4$ with decreasing potential; scan rate is 0.1 mV/s.

attributed definitely to the $LiCoO_2$ electrode and the others are ascribed to the sapphire optical window and the PC containing 1 M $LiClO_4$ [5].

It was found that the Raman intensity for the A_{1g} and E_g modes indicated a remarkable potential dependence, and we focused on the variation of these Raman lines with electrode potential. These lines were fitted by Gaussian curves to clarify the potential dependence in detail, and the peak parameters were determined precisely. Figs. 5 and 6 represent the potential dependences of (a) frequency of the Raman shift (cm^{-1}), (b) the line width (FWHM (cm^{-1})) and (c) the scattering intensity (arb. units) for the A_{1g} and E_g modes. Open circles represent the values obtained for the positive potential scan and the solid circles are for the negative scan.

The frequency of the Raman line of the A_{1g} mode (485 cm^{-1} at 3.1 V) is almost independent of the potential. Only a slight down-shift ($\sim$4 cm^{-1}) was observed when the potential was scanned from 4.0 to 4.2 V in the positive scan and from 3.7 to 3.6 V in the negative scan. Any significant change of the line width was not observed both for the positive and the negative scans. On the other hand, it was confirmed that the electrode potential greatly affects the Raman intensity of the A_{1g} and the E_g modes as shown in Fig. 5(c) and Fig. 6(c). In the positive scan, the Raman intensity suddenly

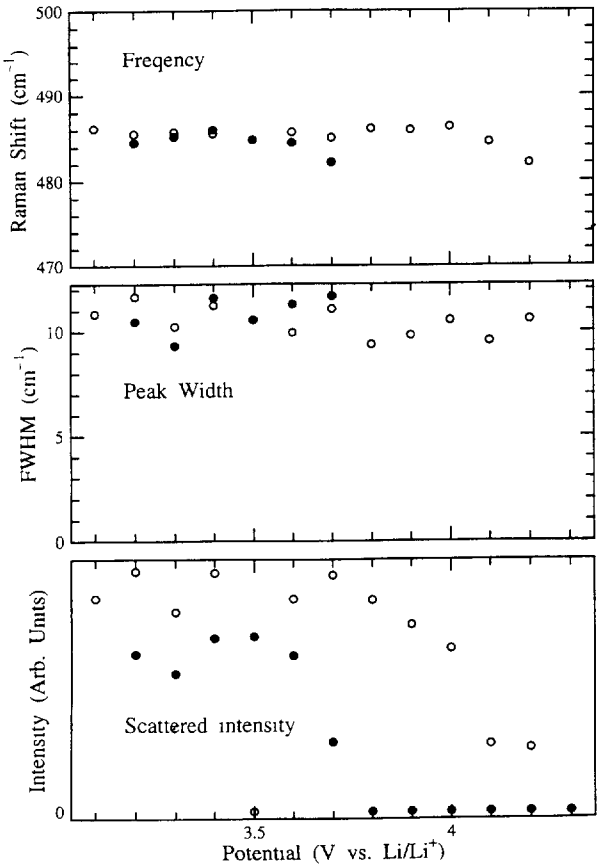

Fig. 5 Effect of the electrode potential on (a) the peak frequency (cm^{-1}), (b) the line width (cm^{-1}) and (c) the scattering intensity (arb. units) of the Raman lines of the A_{1g} vibration (485 cm^{-1}). Solid and open circles represent values obtained for increasing and decreasing potential, respectively.

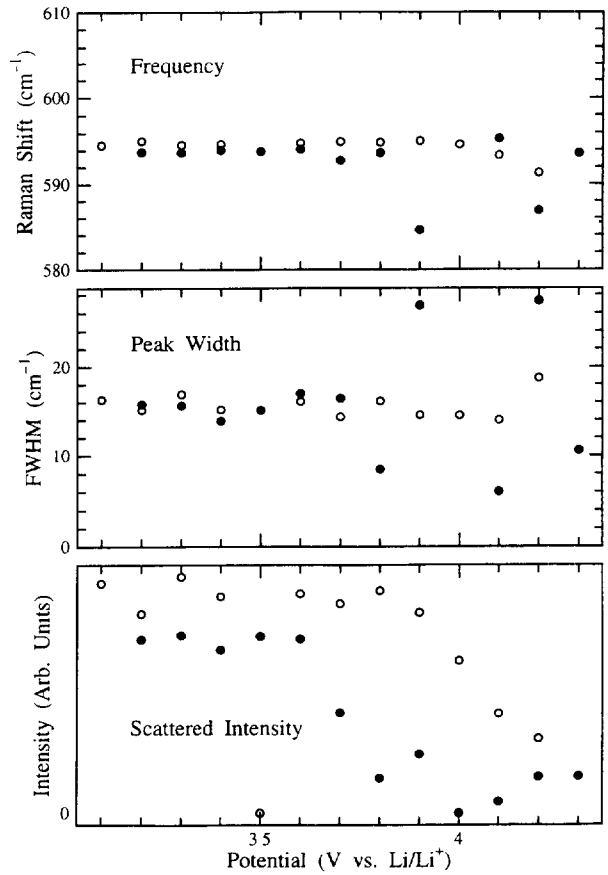

Fig. 6. Effect of the electrode potential on (a) the peak frequency (cm^{-1}), (b) the line width (cm^{-1}) and (c) the scattering intensity (arb. units) for the Raman lines of the E_g vibration (597 cm^{-1}). Solid and open circles represent values obtained for increasing and decreasing potential, respectively

decreased at 3.9 V, but it certainly recovered at 3.7 V in the negative scan. This potential dependence is discussed in the next section.

4. Discussion

The in situ Raman spectroscopic measurements revealed that the Raman scattering intensity of Li_xCoO_2 depends on the applied potential, where the Li^+-ion extraction/insertion takes place electrochemically.

A possible explanation for this finding is that the decrease in Raman intensity is derived from an increased electrical conductivity of Li_xCoO_2. Shibuya et al. [15] carried out in situ conductivity measurements of Li_xCoO_2 during electrochemical extraction/insertion of Li^+ ions in organic solvents using interdigitated microarray electrodes. According to them, the electronic conductivity of Li_xCoO_2 increases two orders of magnitude at least with increasing the potential during Li^+-ion extraction from 3.0 to 4.2 V versus Li/ Li^+. When the potential is close to 3.9 V, the increased conductivity becomes saturated. The decrease in Raman intensity observed at potentials more positive than 3.8 V is well corresponding to the conductivity change.

The electrical conductivity is directly related to the optical skin depth (δ) of the laser beam

$$\delta = \sqrt{\frac{2}{\mu\sigma\omega}} \quad (1)$$

where μ, σ and ω are the magnetic permeability, the electronic conductivity and the inverse of the wavelength, respectively. Increase in electronic conductivity will result in reduction of the optical skin depth. When the potential becomes more positive than 3.8 V, the conductivity becomes correspondingly large, and the penetration depth of incident laser beam becomes smaller and smaller. Since the incident laser picks up the information near the shallow surface region of the Li_xCoO_2 film, and the resultant scattering intensity decreases largely in the positive scan and vice versa in the negative scan. This change is reversible.

Another explanation is possible in consideration of a phase transition of the Li_xCoO_2 structure. It is reported that the lithium intercalation/de-intercalation processes induces a phase transition in the region $0.75 < x < 0.93$ [9] and $0.75 < x < 1$ [10] of Li_xCoO_2 and leads to a disordered struc-

ture. Therefore, a phase transition from Raman-active phase to a Raman-inactive phase is conceivable. If so, we would observe the decrease in Raman scattering intensity associated with de-intercalation. At present, however, rather reasonable one is the former explanation based on the change in skin depth caused by the potential-dependent conductivity change of Li_xCoO_2.

Acknowledgements

This work was supported by Grants-in-Aid for Scientific Research (No. 06 453 111) of The Ministry of Education, Science and Culture, and partly by Asahi Glass Foundation. The authors wish to thank D. Takahashi and S. Waki for their help in the fabrication of the electrodes and Dr T. Maeda of Ishinomaki Senshu University for his useful discussions and comments.

References

[1] R.K. Chang and T.E Furtak (ed.), *Surface Enhanced Raman Scattering*, Plenum, New York, 1982.
[2] R.L. MaCreey, *Electroanal. Chem., 17* (1991) 221–375.
[3] M. Inaba, H. Yoshida, Z. Ogumi, T. Abe, Y. Mizutani and M. Asano, *J Electrochem. Soc., 142* (1995) 20
[4] D.E. Irish, Z. Deng and M. Odziemkowski, *J. Power Sources, 54* (1995) 28
[5] T. Itoh, Y. Matsutani and I. Uchida, *Denki Kagaku, 64* (1996) 76.
[6] H. Tachikawa, *In Situ Raman Spectroscopy of Lithium Electrode Surface in Ambient Temperature Lithium Secondary Battery Final Report*, Lawrence Berkeley Laboratory, CA, USA, 1992.
[7] D. Aurbach, Y. Ein-Ely and A. Zaban, *J. Electrochem. Soc., 141* (1994) L1.
[8] D. Aurbach, A. Zaban, Y Ein-Eli, I. Weissman, O. Chusid, B. Markovsky, M. Levi, E. Levi, A. Schechter and E. Granot, *Ext. Abstr., 8th Int. Meet. Lithium Batteries, 1996*, p. 77.
[9] J.N. Reimers and J.R. Dahn, *J. Electrochem. Soc., 139* (1992) 2091.
[10] T. Ohzuku and A. Ueda, *J. Electrochem Soc., 141* (1994) 2972.
[11] I. Uchida and H. Sato, *J. Electrochem. Soc., 142* (1995) L139.
[12] I. Uchida, H. Hujiyoshi and S. Waki, *Ext. Abstr., 8th Int. Meet. Lithium Batteries, 1996*, p. 129.
[13] R.K. Moore and W.B. White, *J. Am. Ceram. Soc., 53* (1970) 679.
[14] M. Inaba, Y. Todzuka, H. Yoshida, Y Grincourt, A. Tasaka, Y. Tomida and Z. Ogumi, *Chem. Lett.*, (1995) 889.
[15] M. Shibuya, T. Matsue and I Uchida, *J. Eelectrochem. Soc., 143* (1996) 3157.